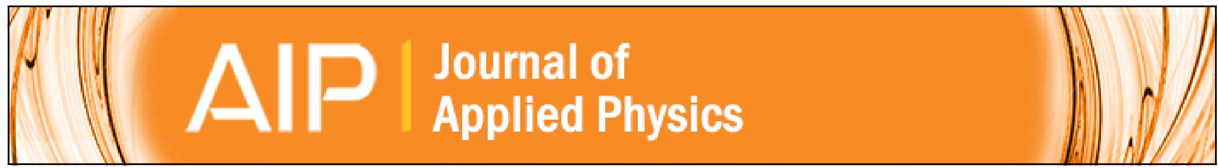

Surface band bending and band alignment of plasma enhanced atomic layer deposited dielectrics on Ga- and N-face gallium nitride

Jialing Yang, Brianna S. Eller, and Robert J. Nemanich

Citation: Journal of Applied Physics **116**, 123702 (2014); doi: 10.1063/1.4895985
View online: http://dx.doi.org/10.1063/1.4895985
View Table of Contents: http://scitation.aip.org/content/aip/journal/jap/116/12?ver=pdfcov
Published by the AIP Publishing

Articles you may be interested in
Band alignment of HfO2/In0.18Al0.82N determined by angle-resolved x-ray photoelectron spectroscopy
Appl. Phys. Lett. **105**, 031602 (2014); 10.1063/1.4891195

Energy band alignment of atomic layer deposited HfO2 oxide film on epitaxial (100)Ge, (110)Ge, and (111)Ge layers
J. Appl. Phys. **113**, 114303 (2013); 10.1063/1.4795284

Comparative band alignment of plasma-enhanced atomic layer deposited high-k dielectrics on gallium nitride
J. Appl. Phys. **112**, 053710 (2012); 10.1063/1.4749268

Energy-band alignment of Al 2 O 3 and HfAlO gate dielectrics deposited by atomic layer deposition on 4 H – SiC
Appl. Phys. Lett. **96**, 042903 (2010); 10.1063/1.3291620

Energy-band parameters of atomic layer deposited Al 2 O 3 and HfO 2 on In x Ga 1 − x As
Appl. Phys. Lett. **94**, 052106 (2009); 10.1063/1.3078399

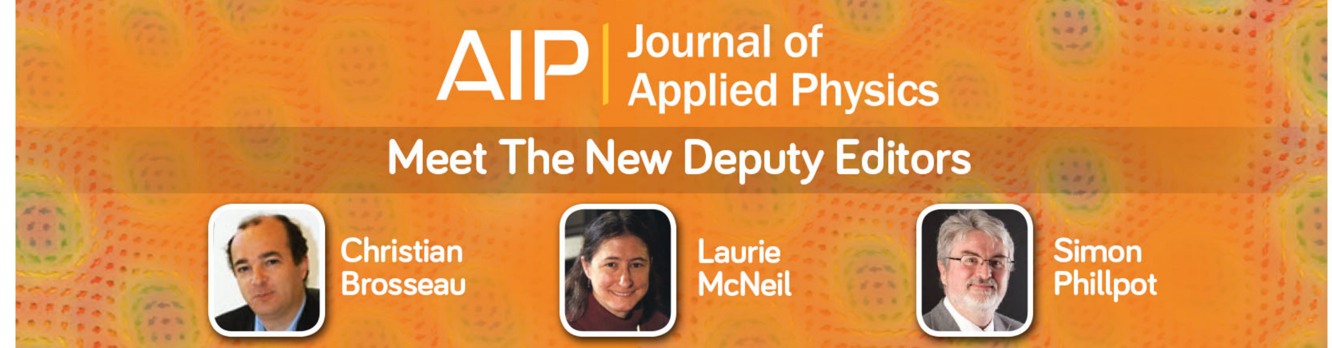

[This article is copyrighted as indicated in the article. Reuse of AIP content is subject to the terms at: http://scitation.aip.org/termsconditions. Downloaded to] IP: 149.169.162.2 On: Tue, 17 Feb 2015 16:58:57

JOURNAL OF APPLIED PHYSICS 116, 123702 (2014)

Surface band bending and band alignment of plasma enhanced atomic layer deposited dielectrics on Ga- and N-face gallium nitride

Jialing Yang, Brianna S. Eller, and Robert J. Nemanich[a)]
Department of Physics, Arizona State University, Tempe, Arizona 85287-1504, USA

(Received 10 June 2014; accepted 6 September 2014; published online 22 September 2014)

The effects of surface pretreatment, dielectric growth, and post deposition annealing on interface electronic structure and polarization charge compensation of Ga- and N-face bulk GaN were investigated. The cleaning process consisted of an *ex-situ* wet chemical NH_4OH treatment and an *in-situ* elevated temperature NH_3 plasma process to remove carbon contamination, reduce oxygen coverage, and potentially passivate N-vacancy related defects. After the cleaning process, carbon contamination decreased below the x-ray photoemission spectroscopy detection limit, and the oxygen coverage stabilized at ~1 monolayer on both Ga- and N-face GaN. In addition, Ga- and N-face GaN had an upward band bending of 0.8 ± 0.1 eV and 0.6 ± 0.1 eV, respectively, which suggested the net charge of the surface states and polarization bound charge was similar on Ga- and N-face GaN. Furthermore, three dielectrics (HfO_2, Al_2O_3, and SiO_2) were prepared by plasma-enhanced atomic layer deposition on Ga- or N-face GaN and annealed in N_2 ambient to investigate the effect of the polarization charge on the interface electronic structure and band offsets. The respective valence band offsets of HfO_2, Al_2O_3, and SiO_2 with respect to Ga- and N-face GaN were 1.4 ± 0.1, 2.0 ± 0.1, and 3.2 ± 0.1 eV, regardless of dielectric thickness. The corresponding conduction band offsets were 1.0 ± 0.1, 1.3 ± 0.1, and 2.3 ± 0.1 eV, respectively. Experimental band offset results were consistent with theoretical calculations based on the charge neutrality level model. The trend of band offsets for dielectric/GaN interfaces was related to the band gap and/or the electronic part of the dielectric constant. The effect of polarization charge on band offset was apparently screened by the dielectric-GaN interface states. © *2014 AIP Publishing LLC*.
[http://dx.doi.org/10.1063/1.4895985]

I. INTRODUCTION

GaN based transistors have shown great potential in high-frequency, high-temperature, and high-power electronic devices due to their relevant material properties, such as large band gap (~3.4 eV), high breakdown field (~3 MV/cm), and high electron saturation velocity (~10^7 cm/s).[1–4] However, device performance has been plagued by a large concentration of surface states, which may lead to leakage current and current collapse.[2,5–8] On the other hand, wurtzite GaN has a significant polarization induced bound sheet charge, which further complicates device reliability. Compared to the large spontaneous polarization ($=-0.033$ C/m^2),[9] the piezoelectric polarization is negligible for GaN typically grown above the critical thickness (~10 nm).[10] The spontaneous polarization leads to a negative or positive bound sheet charge (~2.1×10^{13} charges/cm^2) at the Ga- or N-face, respectively, which must be compensated to avoid a large internal field in the material. Surface states, which may be related to the polarization charge compensation, have a considerable effect on the failure mechanisms. The states may assist thermionic emission and/or thermionic field emission electron tunneling by acting as trapping centers[2,11] or pinning states that affect the Schottky barriers.[5,7] On the other hand, current collapse is ascribed to the formation of a virtual gate, which has been related to a change of the surface states.[8] Through an effective cleaning process, dielectric growth, and post deposition annealing treatment, the related states may be passivated, which could mitigate the failure mechanisms.[2]

The dielectric/GaN interface properties have a significant effect on device performance and stability, and this research will consider three different large band gap dielectric layers: HfO_2, Al_2O_3, and SiO_2. The layers can all be deposited by plasma-enhanced atomic layer deposition (PEALD) at similar temperatures with organo-metallic precursors and remote oxygen plasma. PEALD HfO_2, Al_2O_3, and SiO_2 exhibit a substantial variation in band gap energies (~5.8–8.9 eV) and dielectric constant (~25–3.9), where the thin films are typically amorphous. This research will compare layers of each material deposited on Ga- and N-face GaN to investigate the effect of the polarization charge on band offsets and the relation between the band offsets and dielectric properties, i.e., band gap and dielectric constant.

To accomplish this research, *in-situ* x-ray and ultraviolet photoemission spectroscopy (XPS and UPS) were used to characterize the surface chemistry and electronic structure of PEALD dielectrics on Ga- and N-face GaN in order to investigate the polarization charge screening mechanisms, interface band alignment, and effect of opposite polarization charge on dielectric band offsets. Prior to dielectric growth, GaN surfaces were treated with *ex-situ* and *in-situ* cleaning processes to remove carbon contamination, retain stable oxygen coverage, and potentially passivate N-vacancy related defect states. The surface band bending was measured to investigate the charged surface states and compensation mechanism. The results indicated that the surface band bending of both Ga- and N-face

a)Electronic mail: robert.nemanich@asu.edu

 © 2014 AIP Publishing LLC

[This article is copyrighted as indicated in the article. Reuse of AIP content is subject to the terms at: http://scitation.aip.org/termsconditions. Downloaded to] IP: 149.169.162.2 On: Tue, 17 Feb 2015 16:58:57

GaN was 0.7 ± 0.1 eV after the cleaning processes, which suggested a large concentration of interface states with opposite charge on different surfaces. This large concentration of interface states apparently screens the polarization charge and minimizes the effect of polarization on the band offset between dielectric and GaN.

II. EXPERIMENT

A. GaN surface pretreatment

This study used 1 cm^2 sections of double side polished $\sim$450 μm-thick, bulk GaN grown by hydride vapor phase epitaxy (HVPE). The Si doping density was $\sim 8 \times 10^{17}$ cm^{-3}, which indicated the Fermi level was $\sim$0.1 eV below the conduction band minimum (CBM). The surface pretreatment processes included *ex-situ* wet chemical processes and *in-situ* elevated temperature remote NH_3 plasma processing. The wet chemical clean included sonication in acetone, methanol, and NH_4OH solutions for 10 min each, followed by a 10 s rinse in DI water and blow dry with ultra high purity (UHP) N_2 gas. After the chemical clean, the samples were loaded into the UH vacuum (UHV) system with a base pressure of $\sim 4 \times 10^{-10}$ Torr. Following the *ex-situ* NH_4OH wet chemical clean, the surfaces were processed *in situ* with 15 min NH_3 plasma and 15 min NH_3 gas annealing at 680 °C. The substrate temperature was measured using a thermocouple and infrared pyrometer. The remote plasma was generated by a radio frequency (rf) source (100 W, 13.56 MHz) applied to a helical copper coil wrapped around a $\sim$32 mm diameter quartz tube located $\sim$25 cm above the sample with a constant gas flow of 90 standard cubic centimeters per minute (sccm). Chamber pressure was maintained at 60 mTorr controlled by a throttle valve in front of the turbo pump.

B. PEALD dielectric growth and post deposition annealing

After surface pretreatment, $\sim$1.5 and 3.0 nm PEALD dielectric films (HfO_2, Al_2O_3, and SiO_2) were deposited on Ga- or N-face GaN. The PEALD system has been discussed in detail elsewhere.[12] The precursors used for HfO_2, Al_2O_3, and SiO_2 growth were tetrakis(ethylmethylamido)-hafnium (TEMAHf, $Hf(NCH_3C_2H_5)_4$), dimethylaluminum isoproxide (DMAI, $[(CH_3)_2AlOCH(CH_3)_2]_2$), and tris(dimethylamino)silane (TDMAS, $[(CH_3)_2N]_3SiH$), respectively. The respective TEMAHf, DMAI, and TDMAS bubblers were maintained at 48, 90, and 33 °C to provide sufficient vapor pressure for PEALD deposition. The delivery line temperatures were maintained at $\sim$20 °C higher than that of the specific bubbler to prevent precursor condensation. The PEALD growth rate for HfO_2, Al_2O_3, and SiO_2 films was $\sim$1.4 Å/cycle, $\sim$1.5 Å/cycle, and $\sim$0.5 Å/cycle at respective substrate temperatures of $\sim$220 °C, $\sim$180 °C,[12] and $\sim$200 °C. After dielectric growth, samples were annealed in N_2 ambient at 600 °C for 30 min.

C. X-ray and ultraviolent photoemission spectroscopy characterization

The *in-situ* XPS and UPS systems and measurement approaches have been described previously.[13,14] XPS was used after each cleaning process to investigate the effect of different processes on the GaN chemical states. After dielectric growth, both XPS and UPS were used to characterize the interface electronic structure to determine the GaN surface band bending and band offsets.

The method for determining the valence band offset (VBO) reported by Waldrop and Grant, and Kraut *et al.*[15,16] is represented by the following equation:

$$\Delta E_V = (E_{CL} - E_V)_{GaN} - (E_{CL} - E_V)_{dielectric} + \Delta E_{CL}, \quad (1)$$

where ΔE_V represents VBO; E_{CL} is the binding energy of the XPS core level; E_V is the valence band maximum (VBM); $(E_{CL}\text{-}E_V)_{GaN}$ or $(E_{CL}\text{-}E_V)_{dielectric}$ is the binding energy difference from VBM to GaN or dielectric core level; and ΔE_{CL} is the binding energy difference between the GaN and dielectric core levels, e.g., $\Delta E_{Hf4f7/2\text{-}Ga3d}$ for HfO_2/GaN, $\Delta E_{Al2p\text{-}Ga3d}$ for Al_2O_3/GaN, and $\Delta E_{Si2s\text{-}Ga3d}$ for SiO_2/GaN. The value of $(E_{CL}\text{-}E_V)$ is essentially independent of band bending. Once measured, ΔE_V and band bending can be determined from ΔE_{CL} and the position of the Ga 3d core level, respectively.

III. RESULTS

Using the method described above, surface band bending and/or band alignment for the following samples were determined: cleaned Ga- and N-face GaN, HfO_2/Ga-face GaN, HfO_2/N-face GaN, Al_2O_3/Ga-face GaN, Al_2O_3/N-face GaN, SiO_2/Ga-face GaN, and SiO_2/N-face GaN.

A. Cleaning of Ga- and N-face GaN

Fig. 1 shows the O 1s and C 1s XPS peaks for Ga- and N-face GaN after the different cleaning processes. As-received Ga- and N-face GaN showed similar carbon and oxygen coverage on the surface. After NH_4OH treatment, the intensity of the oxygen peak decreased for both Ga- and N-face GaN, which may be the result of dissolving Ga_2O_3 with NH_4OH.[17] However, there was no obvious decrease in intensity of the carbon peak. (It should be mentioned that additional carbon and oxygen may adsorb on the surface during sample mounting and loading into the UHV transfer line.) After *in-situ* NH_3 plasma treatment, there was a significant decrease in the carbon and oxygen peak intensities on both surfaces. In particular, the intensity of the carbon peak was reduced below the XPS detection limit, and the intensity of the O 1s peak decreased to similar levels on both surfaces. The binding energies of Ga 3d, N 1s, and O 1s core levels for Ga- and N-face GaN are summarized in Table I. A broad O 1s peak centered at 532.6–531.7 eV and 532.8–532.2 eV was detected for both surfaces.

Fig. 2 shows the Ga 3d and UPS results for Ga- and N-face GaN after NH_3 plasma cleaning. The VBM was determined from a linear extrapolation of the UPS low binding energy cutoff. The GaN photo threshold energy was determined from the energy difference between the photon energy (He I = 21.2 eV) and the UPS spectral width (or equivalently, the sum of electron affinity and the band gap of GaN). The photo threshold energy of Ga- and N-face GaN after cleaning was 7.0 ± 0.1 and 6.9 ± 0.1 eV, respectively. Using 3.4 eV as

[This article is copyrighted as indicated in the article. Reuse of AIP content is subject to the terms at: http://scitation.aip.org/termsconditions. Downloaded to] IP: 149.169.162.2 On: Tue, 17 Feb 2015 16:58:57

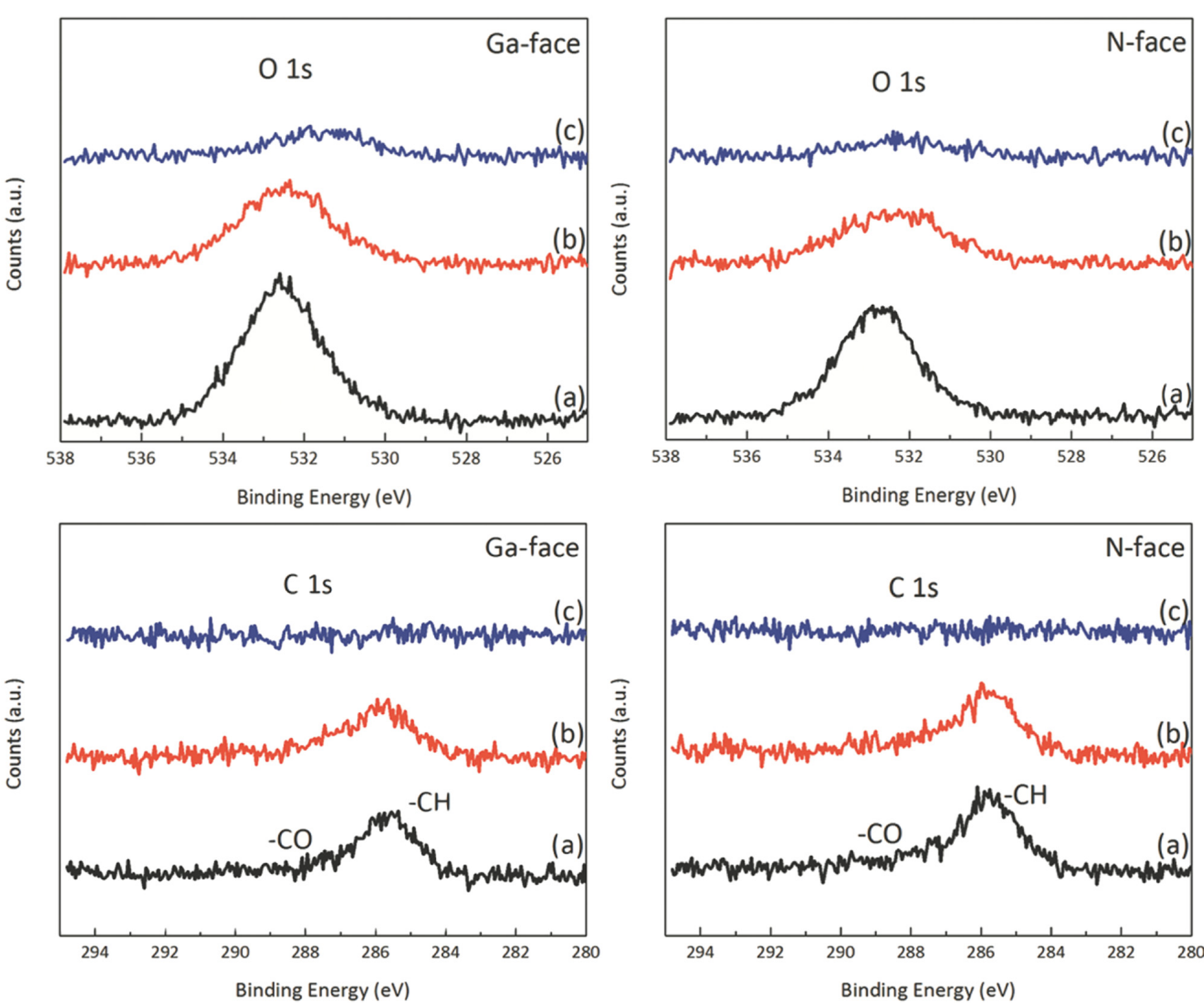

FIG. 1. XPS O 1s and C 1s peaks of (a) as received; (b) *ex-situ* wet chemical treated; and (c) *in-situ* NH_3 plasma treated Ga-face and N-face GaN.

the band gap of GaN, the electron affinity of Ga- and N-face GaN was determined to be 3.6 ± 0.1 and 3.5 ± 0.1 eV, respectively; while these values agreed with other reported results for Ga-face GaN (3.2–3.6 eV),[18–21] they were higher than a previous study of a GaN surface with negligible oxygen coverage (2.8 ± 0.1 eV).[22] The binding energy difference between the Ga 3d core level and VBM for both Ga- and N-face GaN was 17.8 eV, respectively, which was consistent with reported results.[15,23,24] This value was used to determine the surface band bending of GaN. After cleaning, the Ga 3d core level shifted to lower binding energy for both faces, indicating an increase in upward band bending. For Ga-face GaN, the respective upward band bending values after NH_4OH clean and NH_3 plasma treatment were 0.4 and 0.9 eV, and for N-face GaN, the upward band bending was 0.1 and 0.6 eV. These values were consistent with other group's results for Ga-face GaN (0.3–1.5 eV)[13,25–27] and N-face GaN (0.1–1.0 eV).[28–30] Fig. 3 shows a schematic of the surface band bending of Ga- and N-face GaN after *in-situ* NH_3 plasma treatment, where the Ga- and N-face GaN exhibited upward bending of 0.8 ± 0.1 eV and 0.6 ± 0.1 eV, respectively.

TABLE I. XPS results for as-received, wet-chemical cleaned, and NH_3 plasma cleaned Ga- and N-face bulk GaN.

	Ga-face GaN						N-face GaN					
	as received (± 0.1 eV)		wet chemical (± 0.1 eV)		NH_3 plasma (± 0.1 eV)		as received (± 0.1 eV)		wet chemical (± 0.1 eV)		NH_3 plasma (± 0.1 eV)	
	Center	FWHM	Center	FWHM	Center	FWHM	Center	FWHM	Center	FWHM	Center	FWHM
Ga 3d	20.9	1.1	20.7	1.2	20.2	1.2	21.2	1.2	21.0	1.2	20.5	1.3
N 1s	398.2	1.1	398.0	1.1	397.5	1.2	398.6	1.1	398.3	1.0	397.8	1.0
O 1s	532.6	2.4	532.5	2.8	531.7	3.2	532.8	2.3	532.3	3.1	532.2	3.6

[This article is copyrighted as indicated in the article. Reuse of AIP content is subject to the terms at: http://scitation.aip.org/termsconditions. Downloaded to] IP: 149.169.162.2 On: Tue, 17 Feb 2015 16:58:57

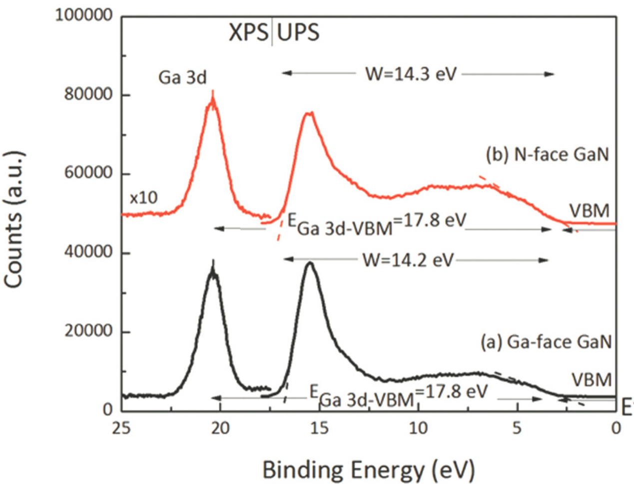

FIG. 2. XPS Ga 3d and UPS results of (a) Ga-face and (b) N-face GaN after NH_3 plasma cleaning. The Ga 3d peak intensity is enlarged 10 times.

B. Surface band bending and band alignment of HfO_2/Ga- and N-face GaN

After surface pretreatment, ~1.5 and 3.0 nm HfO_2 films were deposited on both Ga- and N-face GaN by PEALD and annealed in a N_2 atmosphere at 600 °C. Since the Hf 4f peaks overlap with the Ga 3d peak and the binding energy difference between Ga 3d and N 1s core level is constant, the N 1s core level was used to locate the Ga 3d peak position. Fig. 4 shows the XPS Hf 4f, Ga 3d, and N 1s core levels of PEALD HfO_2 on both Ga- and N-face GaN. After ~1.5 nm HfO_2 deposition and annealing, Ga- and N-face GaN exhibited respective Ga 3d core level binding energies of 20.5 and 20.7 eV, which indicated upward band bending of 0.6 and 0.4 eV. The respective Hf $4f_{7/2}$ peak of HfO_2 was centered at 17.9 and 18.1 eV on Ga- and N-face GaN, which indicated the $\Delta E_{Hf4f7/2\text{-}Ga3d}$ was −2.6 eV. The value of $(E_{Hf4f7/2}\text{-}E_V)_{HfO2}$ was calculated from the binding energy difference between the XPS Hf $4f_{7/2}$ core level and the UPS HfO_2 VBM, which is shown in Fig. 5. This value was 13.7 eV for as-grown and annealed HfO_2 films, which was consistent with our previous study (13.6–13.7 eV)[13] and other research

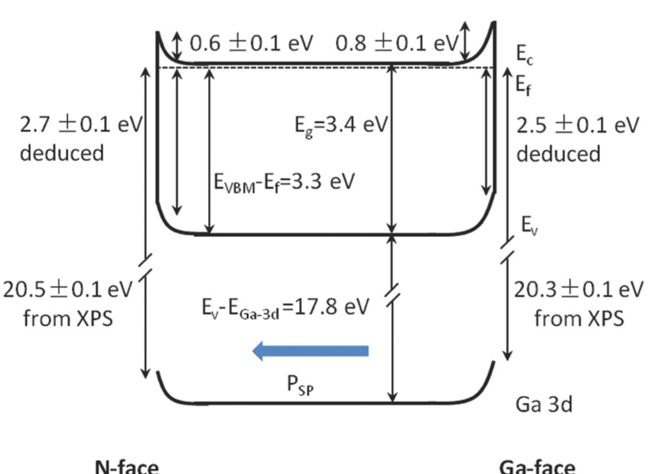

FIG. 3. Surface band bending diagram of Ga- and N-face GaN after NH_3 plasma cleaning.

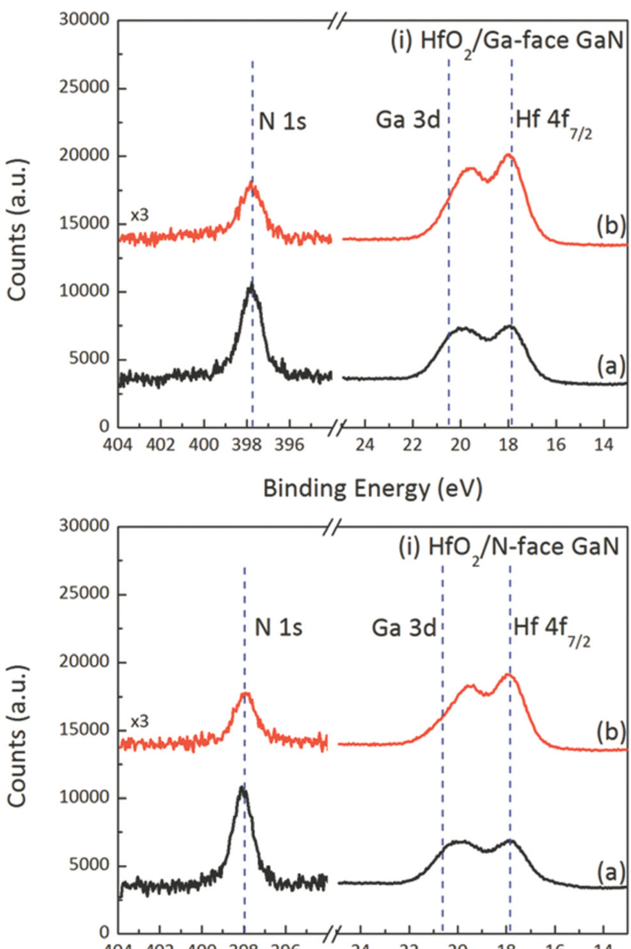

FIG. 4. XPS Hf 4f, Ga 3d, and N 1s core levels of PEALD HfO_2 on both (i) Ga- and (ii) N-face GaN for (a) ~1.5 nm and (b) 3.0 nm annealed HfO_2. The final positions of the core level peaks after HfO_2 growth are indicated with dashed lines. The intensity of N 1s core level is enlarged 3 times. The N 1s core level is used to locate the Ga 3d peak position, which overlaps with Hf 4f double peaks by assuming the binding energy difference between Ga 3d and N 1 s core level is constant.

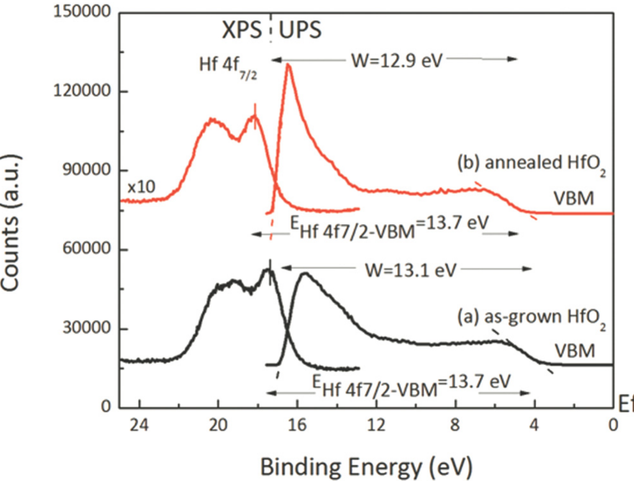

FIG. 5. XPS Hf 4f and UPS results of (a) as-grown and (b) annealed PEALD HfO_2 on N-face GaN. The XPS signal intensity is enlarged 10 times.

[This article is copyrighted as indicated in the article. Reuse of AIP content is subject to the terms at: http://scitation.aip.org/termsconditions. Downloaded to] IP: 149.169.162.2 On: Tue, 17 Feb 2015 16:58:57

TABLE II. XPS Ga 3d, N 1s, and Hf $4f_{7/2}$ core levels, and VBO results for HfO_2 on Ga- and N-face GaN. All energies are given in eV.

	Ga 3d		N 1s		Hf $4f_{7/2}$		VBO	
Process	Ga-face	N-face	Ga-face	N-face	Ga-face	N-face	Ga-face	N-face
(a) After clean	20.3	20.5	397.5	397.8	…	…	…	…
(b) 1.5 nm HfO_2	20.5	20.7	397.8	398.0	17.9	18.1	1.5	1.5
(c) 3.0 nm HfO_2	20.5	20.6	397.8	397.9	17.9	17.9	1.5	1.4

(13.9 eV).[31] The same value of $(E_{Hf4f7/2}\text{-}E_V)_{HfO2}$ was obtained for Ga-face GaN, which is not shown. Therefore, the value of $(E_{Hf4f7/2}\text{-}E_V)_{HfO2}$ was determined to be 13.7 eV, which was used for the band offset calculation. By using Eq. (1) and 5.8 eV as the HfO_2 band gap, the respective VBO and CBO were 1.5 and 0.9 eV on both Ga- and N-face GaN.

After an additional 1.5 nm HfO_2 deposition and annealing, the Ga 3d and Hf $4f_{7/2}$ peaks were centered at 20.5 and 17.9 eV for Ga-face GaN, and 20.6 and 17.9 eV for N-face GaN, respectively. The value of $\Delta E_{Hf4f7/2\text{-}Ga3d}$ was -2.6 and -2.7 eV, and the subsequent VBO was calculated to be 1.5 and 1.4 eV for HfO_2 on Ga- and N-face GaN. The related Ga 3d, N 1s, and Hf $4f_{7/2}$ core levels, and the VBO results are summarized in Table II. The photo threshold energy for HfO_2 on GaN was 8.2 ± 0.1 eV, and the electron affinity was calculated to be 2.4 ± 0.1 eV; these values were consistent with our previous result (2.2 eV)[13] and also close to the value of 2.5 eV reported by Bersch *et al.*[32] The band alignment diagrams of HfO_2 on Ga- and N-face GaN are shown in Fig. 6. The VBO and CBO of HfO_2 on GaN were 1.4 ± 0.1 eV and 1.0 ± 0.1 eV, independent of GaN polarities and HfO_2 thickness.

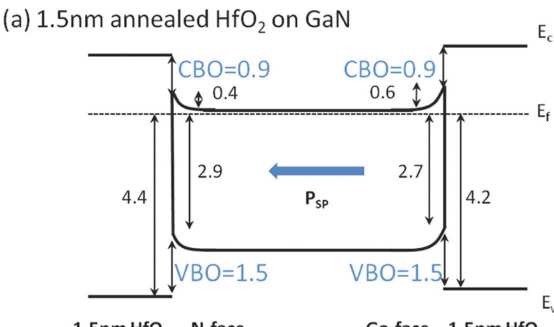

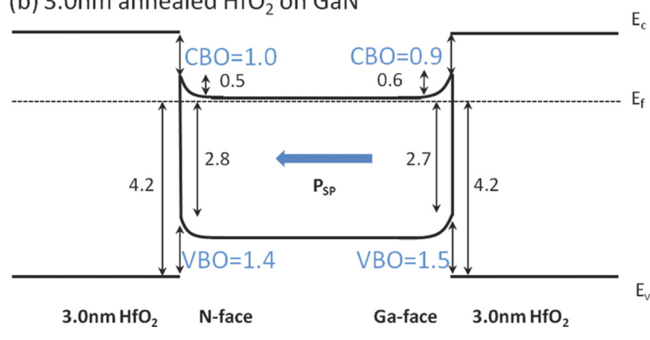

FIG. 6. The deduced band alignment of (a) ~1.5 nm and (b) 3.0 nm annealed HfO_2 on Ga- and N-face GaN.

C. Surface band bending and band alignment of Al_2O_3/Ga- and N-face GaN

Similar to the HfO_2/GaN study, ~1.5 and 3.0 nm Al_2O_3 films were deposited on Ga- and N-face GaN and annealed at 600 °C in a N_2 atmosphere. Fig. 7 shows the Al 2p and Ga 3d XPS core levels of ~1.5 and 3.0 nm Al_2O_3 on Ga- and N-face GaN (i and ii, respectively). The XPS core level binding energies and VBM results are summarized in Table III. For 1.5 nm Al_2O_3 films on Ga-face GaN, the Ga 3d core level was at 21.0 eV, which indicated the GaN VBM at 3.2 eV below E_F and surface band bending of 0.1 eV. The Al 2p core level was centered at 75.9 eV, and the subsequent value of $\Delta E_{Al2p\text{-}Ga3d}$

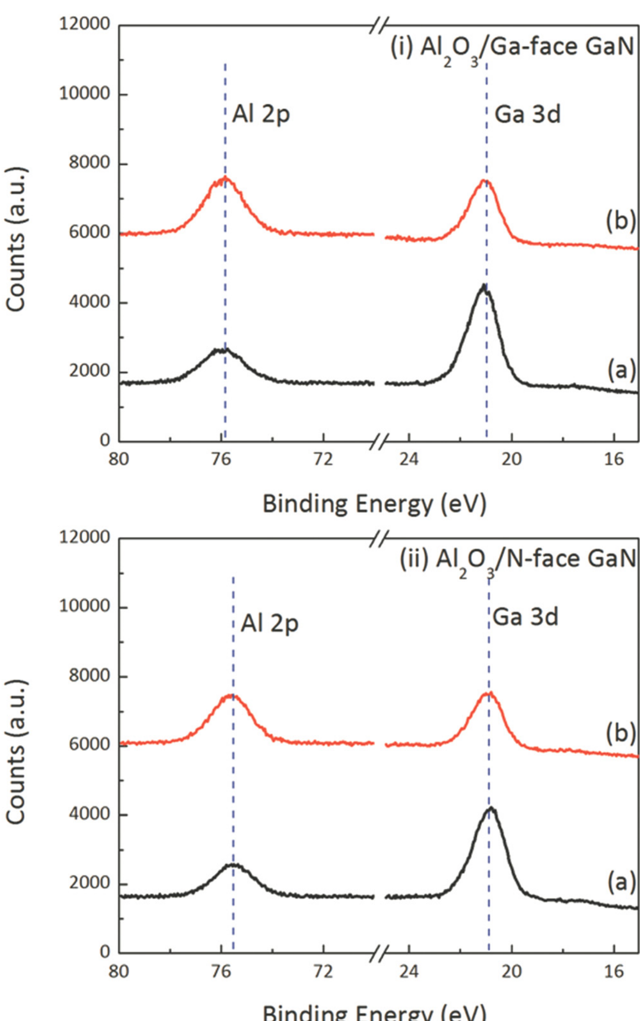

FIG. 7. XPS Ga 3d and Al 2p core levels of Al_2O_3 on (i) Ga- and (ii) N-face GaN for (a) ~1.5 nm and (b) ~3.0 nm annealed Al_2O_3. The final positions of the core level peaks after Al_2O_3 growth are indicated with dashed lines.

[This article is copyrighted as indicated in the article. Reuse of AIP content is subject to the terms at: http://scitation.aip.org/termsconditions. Downloaded to] IP: 149.169.162.2 On: Tue, 17 Feb 2015 16:58:57

TABLE III. XPS Ga 3d, and Al 2p core levels and VBO results for Al_2O_3 on Ga- and N-face GaN. All energies are given in eV.

	Ga 3d		Al 2p		VBO	
Process	Ga-face	N-face	Ga-face	N-face	Ga-face	N-face
(a) After clean	20.5	20.5	…	…	…	…
(b) 1.5 nm Al_2O_3	21.0	20.8	75.9	75.5	2.1	1.9
(c) 3.0 nm Al_2O_3	21.0	20.9	75.9	75.6	2.1	1.9

was 54.9 eV. The value of $(E_{Al2p}\text{-}E_V)_{Al2O3}$ was ~70.6 eV for as-grown and annealed Al_2O_3, which is shown in Fig. 8. The same value of $(E_{Al2p}\text{-}E_V)_{Al2O3}$ (70.6 eV) was obtained on Ga-face GaN, which is not shown. Therefore, 70.6 eV was used as the value of $(E_{Al2p}\text{-}E_V)_{Al2O3}$ in the band offset calculations, which is consistent with our previous study (70.4–70.5 eV)[13] and another group's report (70.6 eV).[32] Using Eq. (1), the VBO between as-grown Al_2O_3 and Ga-face GaN was calculated to be 2.1 eV. After an additional ~1.5 nm Al_2O_3 deposition and annealing in N_2 atmosphere, the ~3.0 nm Al_2O_3/Ga-face GaN showed the same Al 2p and Ga 3d core level energies, which indicated the VBO did not change. For 1.5 nm Al_2O_3 on N-face GaN, the GaN surface band bending was ~0.3 eV upwards, and the value of $\Delta E_{Al2p\text{-}Ga3d}$ was 54.7 eV. For 3.0 nm Al_2O_3 on N-face GaN, these values were essentially unchanged at 0.2 and 54.7 eV, respectively. Therefore, the VBO was 1.9 eV for both cases.

Band gaps of Al_2O_3 and GaN (3.4 eV) are necessary to calculate the conduction band offset (CBO). A previous study from our group reported the band gap of PEALD Al_2O_3 as 6.7 ± 0.1 eV, which was determined from XPS O 1s energy loss spectroscopy.[12] The result is consistent with other results.[33,34] Using 6.7 eV as the band gap of the Al_2O_3 films, the respective CBO was ~1.2 and 1.4 eV for Al_2O_3 on Ga- and N-face GaN, respectively. The deduced band alignment diagrams of Al_2O_3 films on Ga- and N-face GaN are shown in Fig. 9. The VBOs for Al_2O_3 on Ga- and N-face GaN were similar, which were 2.0 ± 0.1 eV and independent of dielectric thickness. This value is consistent with our previous result for Al_2O_3 on Ga-face GaN films (=1.8 ± 0.1 eV).[13]

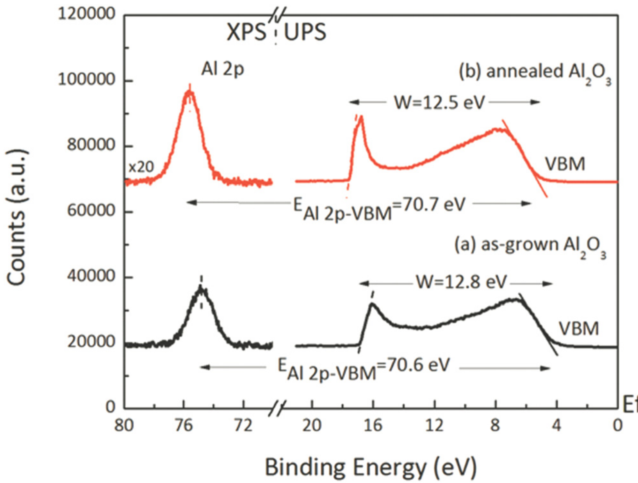

FIG. 8. XPS Al 2p and UPS results of (a) as-grown and (b) annealed PEALD Al_2O_3 on N-face GaN. The XPS signal intensity is enlarged 20 times.

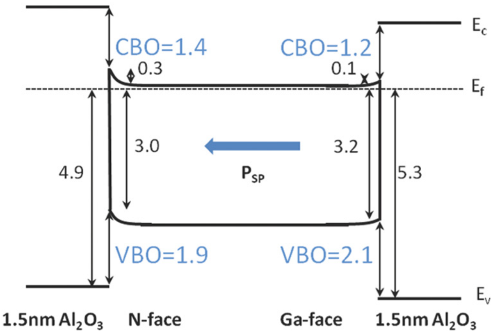

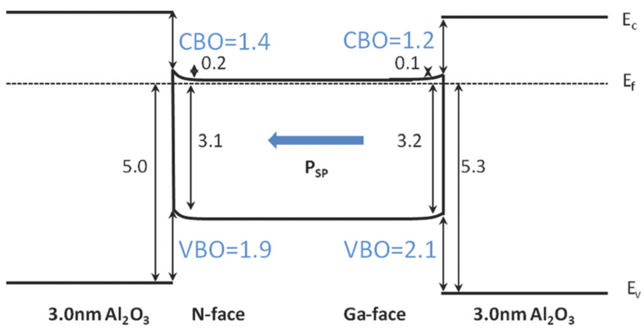

FIG. 9. The deduced band alignment of (a) ~1.5 nm and (b) ~3.0 nm annealed Al_2O_3 on Ga- and N-face GaN.

The photo threshold energies for Al_2O_3/Ga- and N-face GaN measured by UPS were 8.6 ± 0.2 eV. These values indicated the electron affinity of Al_2O_3 films was 1.9 ± 0.2 eV, which is consistent with our previous study (1.8 eV)[13] and other results (1.7 eV).[35]

D. Surface band bending and band alignment of SiO_2/Ga- and N-face GaN

To characterize PEALD SiO_2 on GaN, ~1.5 and 3.0 nm SiO_2 films were deposited on both Ga- and N-face GaN with the same experimental sequence used for HfO_2 and Al_2O_3.

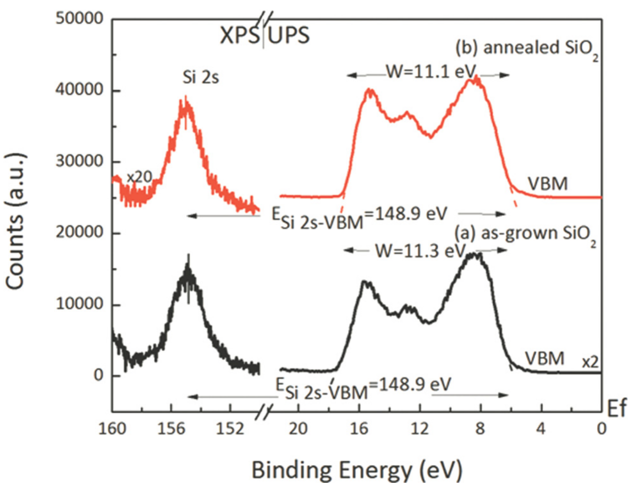

FIG. 10. XPS Si 2s and UPS results of (a) as-grown and (b) annealed PEALD SiO_2 on N-face GaN. The XPS signal intensity and was enlarged by 20 times, and the UPS signal intensity for as-grown SiO_2 is enlarged 2 times.

[This article is copyrighted as indicated in the article. Reuse of AIP content is subject to the terms at: http://scitation.aip.org/termsconditions. Downloaded to] IP: 149.169.162.2 On: Tue, 17 Feb 2015 16:58:57

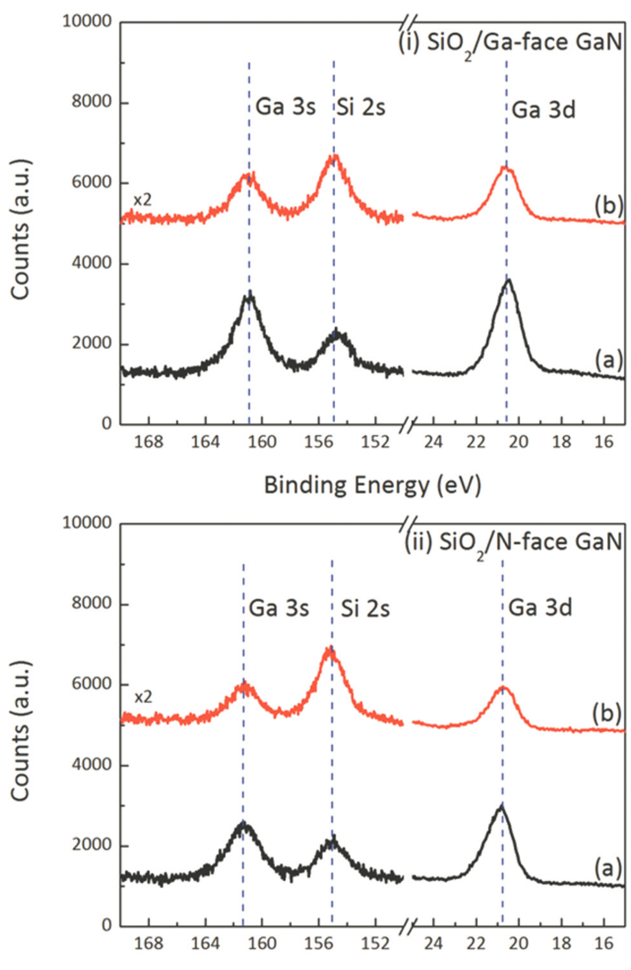

FIG. 11. XPS Ga 3s, Si 2s, and Ga 3d core levels of PEALD SiO_2 on both (i) Ga- and (ii) N-face GaN for (a) ~1.5 nm and (b) 3.0 nm annealed SiO_2. The final positions of the core level peaks after SiO_2 growth are indicated with dashed lines. The XPS Ga 3d and Si 2s peak intensity is enlarged 2 times.

Since the Si 2p peak overlaps with the Ga 3p peaks, the Si 2s core level was measured to indicate the band offset. To obtain both Ga 3s (~160 eV) and Si 2s peaks (~155 eV), the Al source was used to avoid Ga Auger features, which occur in this energy range with the Mg anode.

Fig. 10 shows the XPS Si 2s and UPS results of as-grown and annealed SiO_2 on N-face GaN. The respective peaks centered at ~8 and 13 eV were characteristic of the O (2p) and Si-O related features.[36] From UPS, the electron affinity of SiO_2 on GaN was determined to be 1.1 ± 0.1 eV, which is consistent with a prior study (1.1 eV)[37] and another group's result (1.3 eV).[32] The value of $(E_{Si2s}\text{-}E_V)_{SiO2}$ was calculated as 148.9 eV. The same value was obtained from SiO_2/Ga-face GaN, which is not shown. Therefore, the value of $(E_{Si2s}\text{-}E_V)_{SiO2}$ was determined to be 148.9 eV for the following calculations.

Fig. 11 shows the XPS of the Ga 3s, Si 2s, and Ga 3d core levels of SiO_2 on both Ga- and N-face GaN. After ~1.5 nm SiO_2 deposition and annealing, the Ga 3d of Ga- and N-face GaN was centered at 20.5 and 20.8 eV, respectively, indicating upward band bending of 0.6 and 0.3 eV. The Si 2s peak of SiO_2 was located at 154.7 and 155.0 eV, respectively. Therefore, the value of $\Delta E_{Si2s\text{-}Ga3d}$ was 134.2 eV for both SiO_2/Ga- and N-face GaN. Using Eq. (1) and 8.9 eV as the band gap of SiO_2, the respective VBO and CBO of SiO_2 on both Ga- and N-face GaN were 3.1 and 2.4 eV. After an additional ~1.5 nm SiO_2 deposition and annealing, the Ga 3d core levels of Ga- and N-face GaN changed to 20.6 and 20.7 eV, which indicated 0.5 and 0.4 eV upward band bending, respectively. In addition, the Si 2s core level of SiO_2 on Ga- and N-face GaN were 154.9 and 155.1 eV, respectively. Therefore, the VBOs of 3.0 nm SiO_2/Ga- and N-face GaN were 3.2 and 3.3 eV, respectively. The Ga 3d, Ga 3s, and Si 2s binding energy values and VBO results are summarized in Table IV. The band alignment diagram of SiO_2 on Ga- and N-face GaN is shown in Fig. 12. The respective VBO and CBO of SiO_2 on Ga- and N-face GaN were 3.2 ± 0.1 and 2.3 ± 0.1 eV.

IV. DISCUSSION

Surface states play a critical role in compensating the polarization bound sheet charge and subsequently affecting the surface band bending. In addition, band offsets determine the carrier confinement properties in the semiconductor. Therefore, it is necessary to understand the polarization charge compensation mechanism and the effect of polarization charge on band offsets.

A. Surface composition and oxygen coverage

The surface atomic concentration on Ga- and N-face GaN measured by XPS during the cleaning process is shown in Figs. 13(a) and 13(b). The atomic composition was calculated using the following equation:

$$\eta_x = \frac{I_x/S_x}{I_{Ga}/S_{Ga} + I_N/S_N + I_O/S_O + I_C/S_C}, \tag{2}$$

where $I_{Ga,N,O,C}$ are the integrated area intensities of the respective XPS Ga 3d, N 1s, O 1s, and C 1s peaks; $S_{Ga,N,O,C}$ are the atomic sensitive factors for the respective Ga 3d, N 1s, O 1s, and C 1s photoelectrons, which are 0.31, 0.42, 0.66, and 0.25;[38] and η_x is the atomic concentration of element x.

TABLE IV. XPS Ga 3d, Ga 3s, and Si 2s core levels, and VBO results for SiO_2 on Ga- and N-face GaN. All energies are given in eV.

	Ga 3d		Ga 3s		Si 2s		VBO	
Process	Ga-face	N-face	Ga-face	N-face	Ga-face	N-face	Ga-face	N-face
(a) After clean	20.4	20.4	160.8	160.9	…	…	…	…
(b) 1.5 nm SiO_2	20.5	20.8	161.0	161.3	154.7	155.0	3.1	3.1
(c) 3.0 nm SiO_2	20.6	20.7	161.0	161.2	154.9	155.1	3.2	3.3

[This article is copyrighted as indicated in the article. Reuse of AIP content is subject to the terms at: http://scitation.aip.org/termsconditions. Downloaded to] IP: 149.169.162.2 On: Tue, 17 Feb 2015 16:58:57

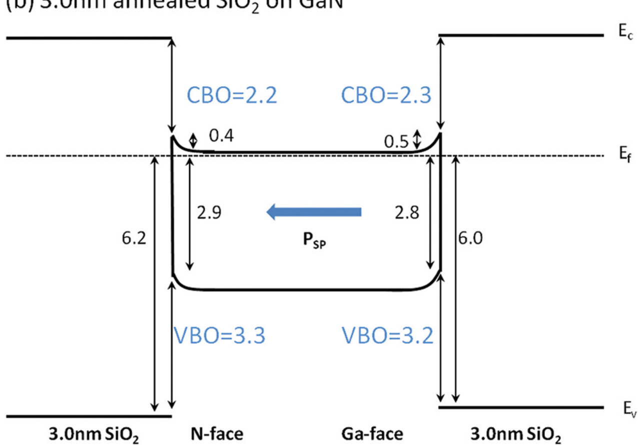

FIG. 12. The deduced band alignment of (a) ∼1.5 nm and (b) 3.0 nm annealed SiO_2 on Ga- and N-face GaN.

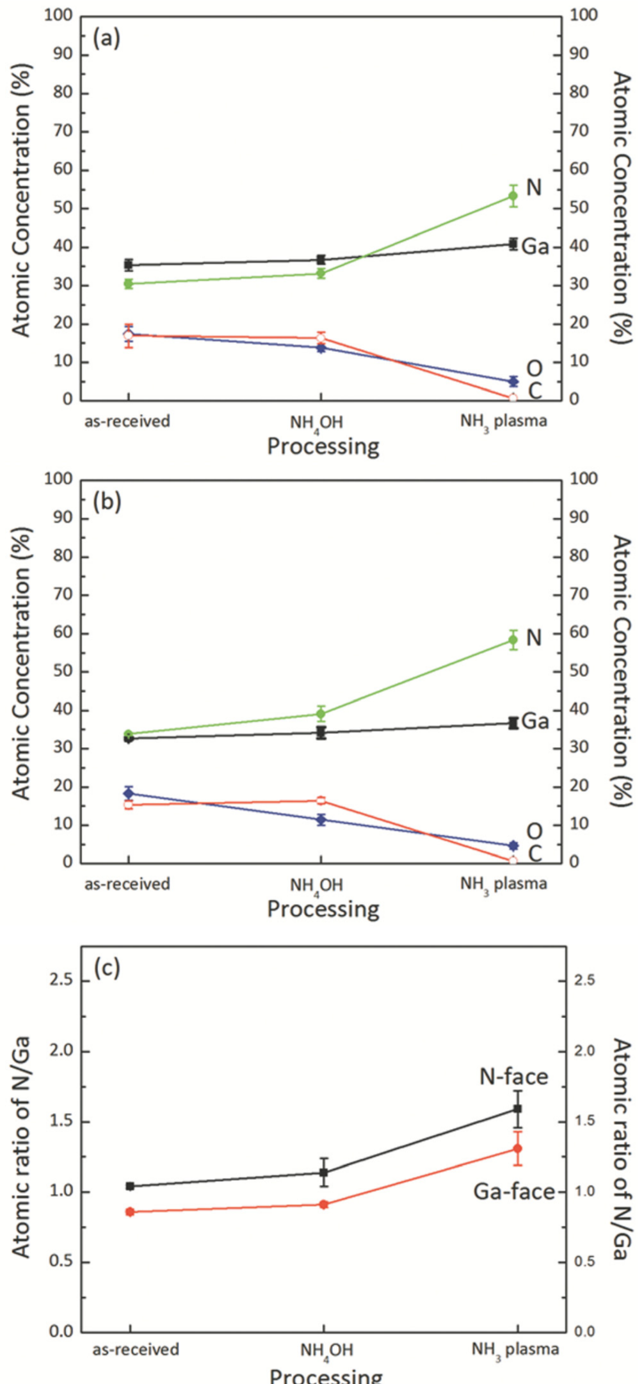

FIG. 13. The atomic concentration of Ga (square), N (circle), O (diamond), and C (hollow circle) of (a) Ga-face and (b) N-face bulk GaN, and (c) the atomic ratio of N to Ga for Ga-face (square) and N-face (circle) GaN during the cleaning processes.

After cleaning, the carbon contamination was below the XPS detection limit (<1%), and the oxygen concentration decreased to ∼5% on both Ga- and N-face GaN. The N/Ga atomic ratio on both Ga- and N-face GaN increased after the cleaning processes, which is shown in Fig. 13(c). Compared with NH_4OH cleaning, the NH_3 plasma process further increased the N/Ga atomic ratio probably from introducing NH_x groups on the GaN surface. During these processes, the upward band bending of Ga- and N-face GaN increased, which may indicate the passivation of donor-like N-vacancy related defect states.

The oxygen coverage was determined from XPS measurements,[13,20,39] which are summarized in Table V. After NH_4OH cleaning, the oxygen coverage on Ga- and N-face GaN was 3.4 ± 0.3 and 3.1 ± 0.4 monolayers (ML), respectively. After *in-situ* NH_3 plasma treatment, the oxygen coverage decreased to ∼1.0 ML on both surfaces. Bermudez[39] reported a study concerning oxygen chemisorption on Ga-face GaN and suggested O was bonded to Ga or N in a direction more nearly along the c axis.[39] Elsner *et al.*[40] reported a theoretical calculation regarding O_2 chemisorption on Ga- and N-face GaN. For ideal Ga-face GaN, stable oxygen coverage was ∼0.375 ML, which could increase to 1 ML for oxygen rich conditions (i.e., where the chemical potential of O is equal to that of O_2). This group also reported a possible stable structure at Ga-rich conditions with a Ga surface layer on top of the ideal Ga-face GaN. In this condition, all adsorbed oxygen resided in three-fold coordinated positions,

TABLE V. The oxygen coverage on Ga- and N-face GaN.

Process	Ga-face GaN	N-face GaN
As-received	4.5 ± 0.5 ML	5.1 ± 0.6 ML
NH_4OH clean	3.4 ± 0.3 ML	3.1 ± 0.4 ML
NH_3 plasma clean	1.1 ± 0.2 ML	1.1 ± 0.1 ML

[This article is copyrighted as indicated in the article. Reuse of AIP content is subject to the terms at: http://scitation.aip.org/termsconditions. Downloaded to] IP: 149.169.162.2 On: Tue, 17 Feb 2015 16:58:57

and the corresponding stable oxygen coverage was 1 ML.[40] On the other hand, for N-face GaN, the calculation suggested that there was always 1 ML of Ga atoms bonded to the N terminating atoms.[40–42] The corresponding stable oxygen coverage on N-face GaN was 0.75–1.0 ML depending on the oxygen chemical potential.[40]

In this research, after the NH_3 plasma cleaning process, the experimental oxygen coverage on both Ga- and N-face GaN surface was ~1 ML, which suggested oxygen was bonded to Ga atoms on both Ga- and N-face GaN. The source of oxygen in the annealing chamber may come from the heater, sample holder, quartz tube, the chamber, or the sample itself.

B. Surface band bending and surface states

The polarization bound charge of GaN is expected to be screened by a combination of internal and external charges. For n-type GaN, the external screening may consist of different surface states, including structural defects, surface termination, surface oxides, contaminants, and adsorbates.[43] The internal screening may include ionized donors or free electrons and bulk states. The total of the internal screening charge, external screening charge, and polarization bound charge is expected to be orders of magnitude less than the polarization. The surface band bending is effectively a measure of the internal screening and the space charge layer, which is presumed to be dominated by ionized donors or free electrons for upward or downward band bending, respectively.

Therefore, the effect of surface pretreatment on the polarization charge compensation mechanism was investigated by monitoring the surface band bending. After NH_4OH treatment, the surface band bending for Ga- and N-face GaN were 0.4 ± 0.1 and 0.1 ± 0.1 eV upwards, respectively. After *in-situ* NH_3 plasma treatment, the surface band bending further increased to 0.8 ± 0.1 and 0.6 ± 0.1 eV, respectively. This increase in upward band bending indicates an increase of the internal screening. During the cleaning processes, the surface Fermi level moved towards the VBM and was finally pinned at ~2.5–2.6 eV above VBM, which was close to the GaN charge neutrality level (CNL) (2.3–2.4 eV (Ref. 7 and 44) above VBM). The upward band bending for N-face GaN indicated negatively charged surface states at a higher density than the positive polarization bound charge. Subsequently, ionized donors were required to compensate the excess surface states, leading to the upward band bending. The charge location at Ga- and N-face GaN corresponding to the surface band bending is shown in Fig. 14.

The experimental upward band bending after NH_3 plasma treatment of these samples was close to the value (0.8 eV) reported by Bermudez *et al.*,[39] where the GaN samples were prepared by Ga deposition or 1 keV N_2^+ bombardment followed by 900° C UHV annealing in both cases. This result suggested the surface Fermi level position observed at ~0.8 eV below the bulk position might be caused by a balance between N vacancy (V_N, donor) and Ga vacancy (V_{Ga}, acceptor) defects.[45,46] Further investigation by Long and Bermudez[47] indicated that the Fermi level at the surface was

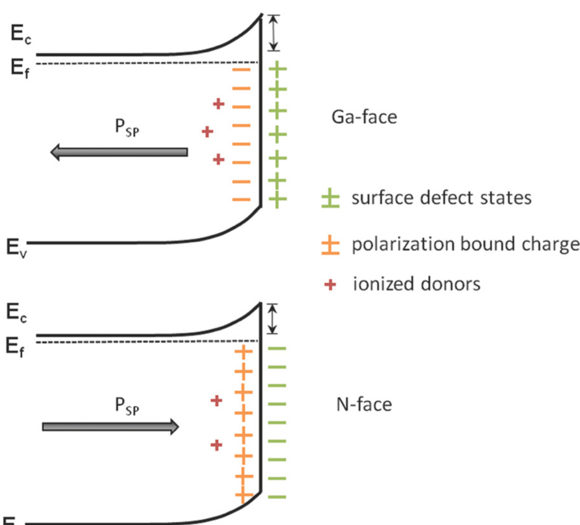

FIG. 14. The surface band bending and charge distribution of Ga- and N-face GaN after cleaning. The number of different charges is not to scale.

~2.55 eV above the VBM for cleaned n- and p-type Ga-face GaN. This value suggested upward band bending of 0.7–0.8 eV on the surface, which was similar to the results reported in this study. The results indicated similar pinning surface states were present regardless of doping type (n- or p- type) and polarities (Ga- or N-face). However, the origin of these pinning states is still not clear.

The relation between the surface potential (Φ_S) and the depletion layer width (W) is given by the following relation:

$$\Phi_S = -\frac{qN_D}{2\varepsilon\varepsilon_o} W^2, \tag{3}$$

where N_D (8×10^{17} cm^{-3}) is the doping density of the bulk GaN; ε (9.5) is the dielectric constant of GaN; and ε_0 (8.854×10^{-12} F/m) is the vacuum permeability. For respective ~0.8 and 0.6 eV upward band bending on Ga- and N-face GaN, the depletion layer width was ~32 and ~28 nm. This depletion region width indicates the area density of ionized donors for Ga- and N-face GaN was $\sim 2.6 \times 10^{12}$ and 2.2×10^{12} charges/cm^2, respectively. The corresponding compensating surface states on Ga- and N-face GaN were $\sim +1.8 \times 10^{13}$ and -2.3×10^{13} charges/cm^2, respectively. The similar internal charge compensation by ionized donors on both faces suggested a similar net charge of surface states and polarization bound sheet charge, which suggested the polarization charge was screened to similar conditions on both faces.

C. Band offsets of dielectrics on GaN

Our previous study compared the experimental band offsets of PEALD HfO_2 and Al_2O_3 on Ga-face GaN with theoretical calculations based on the CNL model.[13] The theoretical VBOs were calculated to be 1.7 and 1.3 eV, respectively, using the following equation:

$$\Delta E_V = E_{CNL,dielectric} - E_{CNL,GaN} - S[I_{GaN} - I_{dielectric} - (E_{CNL,GaN} - E_{CNL,dielectric})], \tag{4}$$

[This article is copyrighted as indicated in the article. Reuse of AIP content is subject to the terms at: http://scitation.aip.org/termsconditions. Downloaded to] IP: 149.169.162.2 On: Tue, 17 Feb 2015 16:58:57

where ΔE_V is the valence band offset; E_{CNL} is the charge neutrality level with respect to the VBM; S is the pinning factor of the wider band gap material; and I is the photo threshold energy. For the SiO_2/GaN VBO calculation, $E_{CNL,SiO2}$ and $E_{CNL,GaN}$ were 4.5 and 2.3 eV with respect to the VBM;[44] S was 0.86 for SiO_2;[48] and I_{GaN} and $I_{dielectric}$ were ~6.9 and 10.0 eV, respectively. Therefore, the VBO for SiO_2 on GaN was calculated to be 3.0 eV. The theoretical calculations for the three dielectrics provided similar agreement to experimental results.

The trend of the dielectric band offsets on GaN vs. band gap is plotted in Fig. 15(a). The figure indicates that to provide a conduction band potential barrier ≥ 1 V to effectively suppress leakage current, the dielectric band gap should be ≥ 5.8 eV. Fig. 15(b) indicates that for the oxides studied here a wider band gap tended to have a smaller dielectric constant. The dielectric constant is a measure of the ability to screen the external electric field. According to the CNL model, the band offset at least partially depends on the Schottky pinning factor, S, of the dielectric, which was related to the electronic part of the dielectric constant (ε_∞).[48] The electronic states are modulated by the high frequency component of the dielectric constant. Therefore, the value of ε_∞ may have a more direct relation with the band offsets than the dielectric constant, as shown in Fig. 15(c). Also shown in Fig. 15(c) is a linear relation between ε_∞ and the reciprocal of the band gap for the three dielectrics studied here. An empirical relation between ε_∞ and band gap is given as follows, which is similar to the equation reported by Reddy:[49]

$$1/E_g = K\varepsilon_\infty + C = Kn^2 + C, \quad (5)$$

where K and C are empirical constants, which are both $\sim 0.034\,\mathrm{eV}^{-1}$ in this study; n is the index of refraction. A similar linear relation was also observed for a number of oxides,[48] in which the value of K and C may be different. To provide the 1 V potential barrier for electrons, the oxide should have an ε_∞ less than 4.0 and a band gap greater than 5.8 eV. All three dielectrics in this study met these requirements. Further study is necessary to establish whether there is a more general trend that would include other oxide dielectrics. Dielectrics with smaller band gaps or higher dielectric constants (or ε_∞) could be alloyed with these dielectrics to adjust the dielectric properties or use these dielectrics as capping and interstitial layers to provide an additional barrier to reduce leakage current.

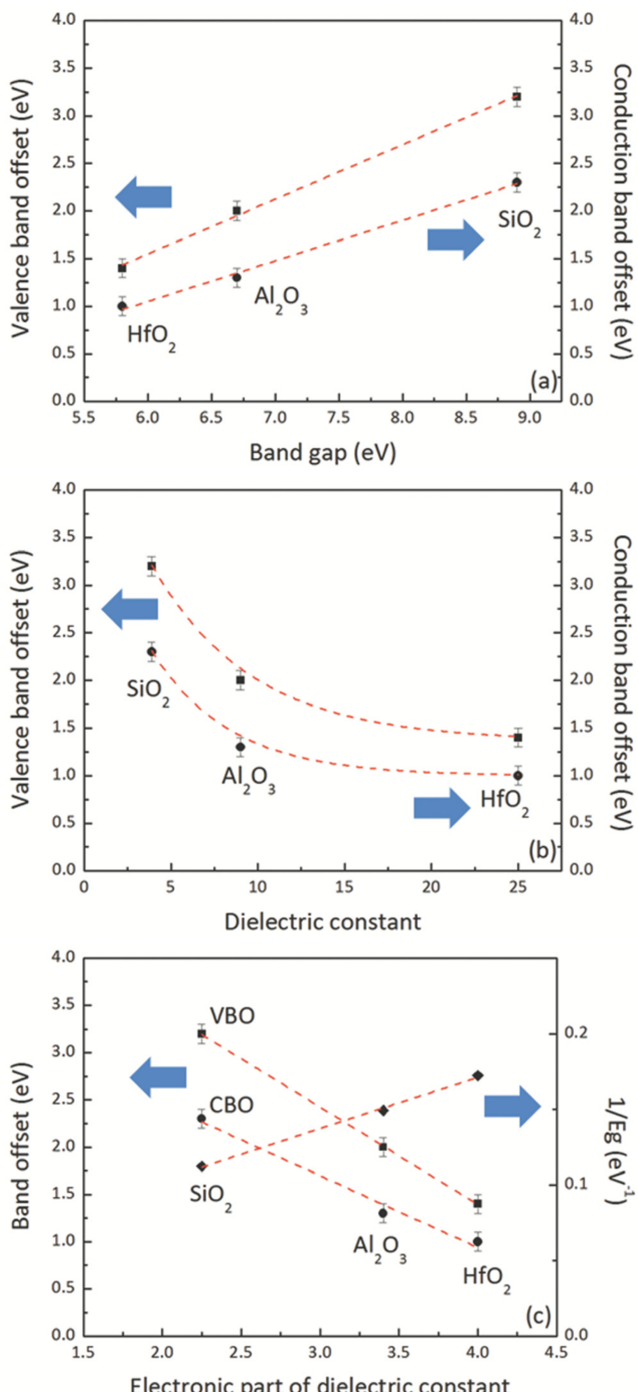

FIG. 15. The relation between band offset of dielectric on GaN and (a) dielectric band gap and (b) dielectric constant; and (c) the relation between electronic part of dielectric constant with band offset and the reciprocal of band gap. The square and circle symbols represent VBO and CBO, respectively. The dashed lines serve as visual aid.

D. Interface dipole and polarization

In this study, the experimental VBO results for HfO_2, Al_2O_3, and SiO_2 on Ga-face GaN were similar to those on N-face GaN. These experimental results are in contrast to measurements of polarization effects at interfaces between two polar crystalline materials such as InN and GaN.[50] In this case as in other polar-polar crystalline interfaces, the interface dipole due to the polarization charge is manifested as an evident change in the VBO for opposite polar configurations. However, the relatively small band bending on Ga- and N-face GaN indicated that the polarization charge is largely screened by a high concentration of interface states. Following the crystalline results, this combination of polarization charge and external screening could be expected to result in an interface dipole of opposite sign for the Ga- and N-face interfaces. The potential drop (ΔV) due to this dipole could be estimated using the following equation:[51]

[This article is copyrighted as indicated in the article. Reuse of AIP content is subject to the terms at: http://scitation.aip.org/termsconditions. Downloaded to] IP: 149.169.162.2 On: Tue, 17 Feb 2015 16:58:57

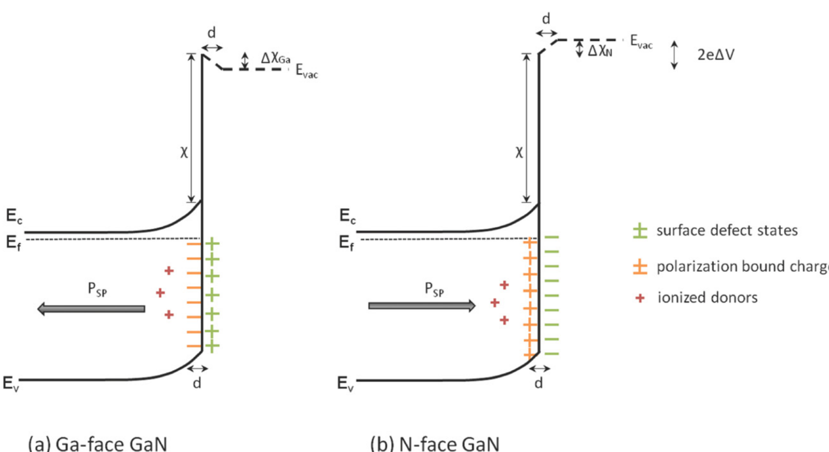

FIG. 16. The energy band diagram of Ga- and N-face GaN after cleaning. $\Delta\chi_{Ga}$ and $\Delta\chi_N$ is the change of electron affinity on Ga- and N-face GaN caused by the electric field between bound sheet charge and surface states. The number of different charges is not to scale.

$$\Delta V = \frac{\sigma}{\varepsilon\varepsilon_0} d, \qquad (6)$$

where σ (3.3×10^{-6} C/cm^2) is the polarization bound charge density; d is the separation between external screening states and polarization bound charge; and ε (9.5) is the dielectric constant of GaN. The potential drop across the dipole would lead to a change of the electron affinity as shown in Fig. 16. Assuming a distance (d) of 2 Å, the potential drop would be ~0.08 V. The subsequent difference in the electron affinity of Ga- and N-face GaN would be ~0.16 eV, which was within the uncertainty of the experimental results (-0.1 ± 0.2 eV). Consequently, the similar electron affinity and band offsets for the Ga- and N-face GaN indicate the external screening should be within several angstroms of the polarization bound charge and the interface dipole did not affect the band offset between dielectrics and GaN. Therefore, similar band offset results could be obtained on both Ga- and N-face GaN.

It is noted that the CNL determination of the VBOs of GaN and dielectric materials did not directly include polarization charge effects.[48] This assumption appears justified within the uncertainty of the results presented here.

V. CONCLUSION

In this research, Ga- and N-face GaN surfaces were cleaned to remove carbon contamination, reduce oxygen coverage, and passivate N-vacancy related defects. After surface pretreatment, both Ga- and N-face GaN were characterized by upward band bending of 0.8 ± 0.1 eV and 0.6 ± 0.1 eV, respectively. The band bending was not obviously correlated with polarization, which suggested a large concentration of compensating surface states. In addition, the cleaning process led to undetectable carbon contamination by XPS and ~1 ML oxygen coverage on both Ga- and N-face GaN, which was consistent with a theoretical calculation that suggested there was 1 ML of Ga atoms on the surface of Ga- or N-face GaN. Three PEALD dielectrics (HfO_2, Al_2O_3, and SiO_2) were deposited on Ga- and N-face GaN to investigate the interface band alignment and effect of polarization charge on the band offsets. The carbon impurities for HfO_2, Al_2O_3, and SiO_2 on GaN were below the XPS detection limit. The respective valence band offsets of HfO_2, Al_2O_3, and SiO_2 on Ga- and N-face GaN were 1.4 ± 0.1, 2.0 ± 0.1, and 3.2 ± 0.1 eV, independent of dielectric thicknesses. Similar VBOs on Ga- and N-face GaN indicated polarization charge was screened by interface states and had little effect on band offsets. The corresponding conduction band offsets were 1.0 ± 0.1, 1.3 ± 0.1, and 2.3 ± 0.1 eV, respectively. These experimental values were consistent with theoretical calculations based on the charge neutrality level model. In addition, the trends of potential barrier for dielectrics on GaN may be related to the dielectric band gap and/or the electronic part of the dielectric constant.

ACKNOWLEDGMENTS

This research was supported by the Office of Naval Research through the DEFINE MURI program, N00014-10-1-0937. We appreciate the helpful discussions with Dr. Tianyin Sun, Manpuneet Kaur, and Xingye Wang.

[1]S. J. Pearton, J. C. Zolper, R. J. Shul, and F. Ren, J. Appl. Phys. **86**, 1 (1999).
[2]B. S. Eller, J. Yang, and R. J. Nemanich, J. Vac. Sci. Technol., A **31**, 050807 (2013).
[3]R. D. Long and P. C. McIntyre, Materials **5**, 1297 (2012).
[4]U. K. Mishra, P. Parikh, and Y. F. Wu, Proc. IEEE **90**, 1022 (2002).
[5]T. Hashizume, J. Kotani, and H. Hasegawa, Appl. Phys. Lett. **84**, 4884 (2004).
[6]E. J. Miller, E. T. Yu, P. Waltereit, and J. S. Speck, Appl. Phys. Lett. **84**, 535 (2004).
[7]H. Hasegawa, T. Inagaki, S. Ootomo, and T. Hashizume, J. Vac. Sci. Technol., B **21**, 1844 (2003).
[8]R. Vetury, N. Q. Zhang, S. Keller, and U. K. Mishra, IEEE Trans. Electron Devices **48**, 560 (2001).
[9]A. Zoroddu, F. Bernardini, P. Ruggerone, and V. Fiorentini, Phys. Rev. B **64**, 045208 (2001).
[10]A. D. Bykhovski, B. L. Gelmont, and M. S. Shur, J. Appl. Phys. **81**, 6332 (1997).
[11]J. C. Carrano, T. Li, P. A. Grudowski, C. J. Eiting, R. D. Dupuis, and J. C. Campbell, Appl. Phys. Lett. **72**, 542 (1998).
[12]J. Yang, B. S. Eller, M. Kaur, and R. J. Nemanich, J. Vac. Sci. Technol., A **32**, 021514 (2014).
[13]J. Yang, B. S. Eller, C. Zhu, C. England, and R. J. Nemanich, J. Appl. Phys. **112**, 053710 (2012).
[14]C. Zhu, S. L. Caudle, J. Yang, D. J. Smith, and R. J. Nemanich, J. Vac. Sci. Technol., B **32**, 011203 (2014).
[15]J. R. Waldrop and R. W. Grant, Appl. Phys. Lett. **68**, 2879 (1996).
[16]E. A. Kraut, R. W. Grant, J. R. Waldrop, and S. P. Kowalczyk, *Heterojunction Band Discontinuities: Physics and Device Applications*, edited by F. Capasso and G. Margaritondo (Elsevier, New York, 1987).

[This article is copyrighted as indicated in the article. Reuse of AIP content is subject to the terms at: http://scitation.aip.org/termsconditions. Downloaded to] IP: 149.169.162.2 On: Tue, 17 Feb 2015 16:58:57

[17]T. Hashizume, S. Ootomo, R. Nakasaki, S. Oyama, and M. Kihara, Appl. Phys. Lett. **76**, 2880 (2000).
[18]C. I. Wu, A. Kahn, N. Taskar, D. Dorman, and D. Gallagher, J. Appl. Phys. **83**, 4249 (1998).
[19]C. I. Wu and A. Kahn, J. Vac. Sci. Technol., B **16**, 2218 (1998).
[20]V. M. Bermudez, J. Appl. Phys. **80**, 1190 (1996).
[21]M. C. Benjamin, M. D. Bremser, T. W. Weeks, S. W. King, R. F. Davis, and R. J. Nemanich, Appl. Surf. Sci. **104/105**, 455 (1996).
[22]K. M. Tracy, W. J. Mecouch, R. F. Davis, and R. J. Nemanich, J. Appl. Phys. **94**, 3163 (2003).
[23]T. E. Cook, Jr., C. C. Fulton, W. J. Mecouch, R. F. Davis, G. Lucovsky, and R. J. Nemanich, J. Appl. Phys. **94**, 7155 (2003).
[24]J. Hedman and N. Mårtensson, Phys. Scr. **22**, 176 (1980).
[25]M. Hong, K. A. Anselm, J. Kwo, H. M. Ng, J. N. Baillargeon, A. R. Kortan, J. P. Mannaerts, A. Y. Cho, C. M. Lee, J. I. Chyi, and T. S. Lay, J. Vac. Sci. Technol., B **18**, 1453 (2000).
[26]Y. Q. Wu, T. Shen, P. D. Ye, and G. D. Wilk, Appl. Phys. Lett. **90**, 143504 (2007).
[27]H. W. Jang, K. W. Ihm, T.-H. Kang, J.-H. Lee, and J.-L. Lee, Phys. Stat. Sol. (b) **240**, 451 (2003).
[28]H. W. Jang, J.-H. Lee, and J.-L. Lee, Appl. Phys. Lett. **80**, 3955 (2002).
[29]P. Lorenz, T. Haensel, R. Gutt, R. J. Koch, J. A. Schaefer, and S. Krischok, Phys. Status Solidi B **247**, 1658 (2010).
[30]V. M. Polyakov, F. S. Tautz, S. Sloboshanin, J. A. Schaefer, A. S. Usikoy, and B. J. Ber, Semicond. Sci. Technol. **13**, 1396 (1998).
[31]S. Suzer, S. Sayan, M. M. B. Holl, E. Garfunkel, Z. Hussain, and N. M. Hamdan, J. Vac. Sci. Technol., A **21**, 106 (2003).
[32]E. Bersch, S. Rangan, R. A. Bartynski, E. Garfunkel, and E. Vescovo, Phys. Rev. B **78**, 085114 (2008).
[33]H. Y. Yu, M. F. Li, B. J. Cho, C. C. Yeo, M. S. Joo, D.-L. Kwong, J. S. Pan, C. H. Ang, J. Z. Zheng, and S. Ramanathan, Appl. Phys. Lett. **81**, 376 (2002).
[34]N. V. Nguyen, O. A. Kirillov, W. Jiang, W. Wang, J. S. Suehle, P. D. Ye, Y. Xuan, N. Goel, K.-W. Choi, W. Tsai, and S. Sayan, Appl. Phys. Lett. **93**, 082105 (2008).
[35]O. Blank, H. Reisinger, R. Stengl, M. Gutsche, F. Wiest, V. Capodieci, J. Schulze, and I. Eisele, J. Appl. Phys. **97**, 044107 (2005).
[36]M. Brause, D. Ochs, J. Günster, T. Mayer, B. Braun, V. Puchin, W. Maus-Friedrichs, and V. Kempter, Surf. Sci. **383**, 216 (1997).
[37]T. E. Cook, Jr., C. C. Fulton, W. J. Mecouch, K. M. Tracy, R. F. Davis, E. H. Hurt, G. Lucovsky, and R. J. Nemanich, J. Appl. Phys. **93**, 3995 (2003).
[38]D. Briggs and M. P. Seah, *Practical Surface Analysis: Auger and X-ray Photoelectron Spectroscopy*, 2nd ed. (John Wiley & Sons, West Sussex, 1990), Vol. 1.
[39]B. S. Eller, J. Yang, and R. J. Nemanich, "Polarization effects of GaN and AlGaN: Polarization bound charge, band bending, and electronic surface states," J. Electron. Mater. (published online).
[40]J. Elsner, R. Gutierrez, B. Hourahine, R. Jones, M. Haugk, and T. Frauenheim, Solid State Commun. **108**, 953 (1998).
[41]A. R. Smith, R. M. Feenstra, D. W. Greve, M. S. Shin, M. Skowronski, J. Neugebauer, and J. E. Northrup, Appl. Phys. Lett. **72**, 2114 (1998).
[42]J. Elsner, M. Haugk, G. Jungnickel, and T. Frauenheim, Solid State Commun. **106**, 739 (1998).
[43]U. Karrer, O. Ambacher, and M. Stutzmann, Appl. Phys. Lett. **77**, 2012 (2000).
[44]W. Mönch, J. Appl. Phys. **109**, 113724 (2011).
[45]V. M. Bermudez, D. D. Koleske, and A. E. Wickenden, Appl. Sur. Sci. **126**, 69 (1998).
[46]J. Neugebauer and C. G. Van de Walle, in *Festkörperprobleme/Advances in Solid State Physics*, edited by R. Helbig (Vieweg, Braunschweig/Wiesbaden, 1996), Vol. 35, p. 25.
[47]J. P. Long and V. M. Bermudez, Phys. Rev. B **66**, 121308 (2002).
[48]J. Robertson and B. Falabretti, J. Appl. Phys. **100**, 014111 (2006).
[49]R. R. Reddy and Y. Nazeer Ahammed, Infrared Phys. Tech. **36**, 825 (1995).
[50]C. Wu, H. Lee, C. Kuo, S. Gwo, and C. Hsu, Appl. Phys. Lett. **91**, 042112 (2007).
[51]W.-C. Yang, B. J. Rodriguez, A. Gruverman, and R. J. Nemanich, Appl. Phys. Lett. **85**, 2316 (2004).

[This article is copyrighted as indicated in the article. Reuse of AIP content is subject to the terms at: http://scitation.aip.org/termsconditions. Downloaded to] IP: 149.169.162.2 On: Tue, 17 Feb 2015 16:58:57